JMEPEG (2012) 21:1937–1942
DOI: 10.1007/s11665-012-0186-3

1059-9495/$19.00

Comparative Study of Hardening Mechanisms During Aging of a 304 Stainless Steel Containing α′-Martensite

S.W. Jeong, U.G. Kang, J.Y. Choi, and W.J. Nam

(Submitted July 9, 2011; in revised form February 2, 2012)

Strain aging and hardening behaviors of a 304 stainless steel containing deformation-induced martensite were investigated by examining mechanical properties and microstructural evolution for different aging temperature and time. Introduced age hardening mechanisms of a cold rolled 304 stainless steel were the additional formation of α′-martensite, hardening of α′-martensite, and hardening of deformed austenite. The increased amount of α′-martensite at an aging temperature of 450 °C confirmed the additional formation of α′-martensite as a hardening mechanism in a cold rolled 304 stainless steel. Additionally, the increased hardness in both α′-martensite and austenite phases with aging temperature proved that hardening of both α′-martensite and austenite phases would be effective as hardening mechanisms in cold rolled and aged 304 stainless steels. The results suggested that among hardening mechanisms, hardening of an α′-martensite phase, including the diffusion of interstitial solute carbon atoms to dislocations and the precipitation of fine carbide particles would become a major hardening mechanism during aging of cold rolled 304 stainless steels.

Keywords aging, austenitic stainless steel, hardening, mechanical property

1. Introduction

A 304 stainless steel is strengthened after plastic deformation not only as a result of work hardening but also of martensitic transformation induced by plastic deformation. It is well known that aging treatment of cold worked metastable austenitic stainless steels, containing strain-induced martensite (α'-martensite) phase, results in the increase of strength, when aging is performed in the temperature range of 200-450 °C (Ref 1-6).

Proposed mechanisms for age hardening in cold worked austenitic stainless steels are (1) the formation of additional α′-martensite (Ref 2-4) and (2) hardening of α′-martensite (Ref 5) or deformed austenite (Ref 6). Mangonon and Thomas (Ref 2) showed that the thermal nucleation of α′-martensite increased tensile strength during aging up to 400 °C. According to Mukhopadhyay et al. (Ref 4), since the precipitation of fine carbides causes the depletion of chromium and carbon in the surrounding matrix, a local increase of the Ms temperature in the surrounding matrix would be responsible for the formation of α′-martensite during cooling after aging treatment. An alternate explanation on aging behavior in stainless steels, containing α′-martensite, was suggested by Rathbun et al. (Ref 5). They did not observe the change in the volume fraction of α′-martensite nor aging behavior in deformed austenite during low temperature aging. Plastically deformed metastable austenitic steels, containing α′-martensite, can be strengthened by the diffusion of interstitial carbon and nitrogen solute atoms to dislocations during aging in the temperature range of 100-400 °C, similar to those observed in low carbon ferritic steels (Ref 7). From the above, it is obvious that age hardening of metastable stainless steels would be closely related to the presence of α'-martensite phase, regardless of proposed age hardening mechanisms. However, it is not still clear yet which mechanism would be most responsible for hardening behavior of cold worked 304 stainless steels during aging.

Thus, to investigate the strain aging and hardening behaviors of a 304 stainless steel containing deformation-induced martensite, the variations of mechanical properties and microstructural evolution with aging temperature and time were examined in the current study. Kinetics of strain aging was also discussed, using the data from differential scanning calorimetry (DSC) curves.

2. Experimental Procedures

The chemical composition of a 304 austenitic stainless steel used in this work was 0.057C, 0.376Si, 1.08Mn, 18.14Cr, 8.14Ni, 0.305Cu, 0.146Mo, and 0.033N (in wt%). An austenite grain size of the hot rolled and annealed sheet was 36.8 μm. To produce strain-induced martensite, steels were cold rolled by 40% (with 16% reduction per pass). Figure 1 shows optical micrographs of stainless steels, (a) annealed and (b) deformed

S.W. Jeong, U.G. Kang, and **W.J. Nam**, School of Advanced Material Engineering, Kookmin University, 861-1 Jeongneung-Dong, Songbuk-Ku, Seoul 136-702, Republic of Korea; and **J.Y. Choi**, Stainless Steel Research Group, POSCO Technical Research Laboratories, POSCO, P.O. Box 36, Pohang 790-785, Republic of Korea. Contact e-mail: wjnam@kookmin.ac.kr.

at a room temperature with 40% reduction. The etching solution for optical microscopy was a mixture of 40 mL HCl and 10 mL HNO_3 for an annealed steel, while a mixture of 0.15 g sodium metabisulfite in 100 mL distilled water and 10 mL HCl in 100 mL distilled water was used for a cold rolled steel. The presence of α′-martensite in a 40% cold rolled steel was confirmed as a dark area indicated in Fig. 1(b).

Microstructure of a cold rolled 304 stainless steel consists of a dispersion of hard martensite in a deformed austenite matrix. Figure 2 shows the typical microstructure of a cold rolled 304 austenitic stainless steel, revealing the bands of twins (diffraction pattern in Fig. 2a) and a small amount of α′-martensite nuclei (marked as a circle in Fig. 2a) formed at the intersections of twins. With increasing the amount of deformation, the density of twins increases (Fig. 2b and c) and the amount of α′-martensite containing high density of dislocations (Fig. 2c) also increases. The amount of α′-martensite calculated from ferritescope readings in a cold rolled steel with 40% reduction was 45.5%.

Aging treatment was performed on cold rolled stainless steel sheets in a heated salt bath in the temperature range of 200-700 °C for an hour. To assess the effect of surface constraint on the transformation response, measurements were performed on steels chemically thinned to remove specific fractions of the sheet thickness. The solution used for surface removal was a mixture of hydrochloric acid, nitric acid, and distilled water in 1:1:1 proportion. The amount of α′-martensite was also measured using ferritescope. Ferritescope readings were converted into the amount of α′-martensite by multiplying with the factor of 1.7, according to Talonen's work (Ref 8).

$$\text{The amount of } \alpha' \text{ - martensite} = 1.71 \times \text{Ferritescope reading} \quad \text{(Eq 1)}$$

Tensile tests were performed at room temperature with a constant displacement speed. The initial strain rate was 6.7×10^{-4}/s. Thermal analysis was performed with a DSC under a flowing Ar atmosphere. As the DSC peak position depends on the heating rate (Ref 9), the measured data of the peak positions for different heating rates of 2-16 °C/min were used. To obtain the activation energy, both the Kissinger (Ref 10) and Chen and Spaepen (Ref 11) methods were applied in this work. To understand the kinetics during heating, stainless steel sheets were heated to the desired temperatures at a rate of 4 °C/min and then rapidly cooled in water. According to the methods, the heating rate (B), the apparent activation energy of the process (Q), and the maximum temperature of the peak T_p are related by the equation

$$\ln(\alpha) = -\frac{Q}{k_B T_p} + C \quad \text{(Eq 2)}$$

where k_B is the Boltzmann's constant and C is an integration constant.

3. Results

3.1 Mechanical Property

Figure 3 shows that the shapes of the stress-strain curves of 304 stainless steels, deformed 40% and subsequently aged in

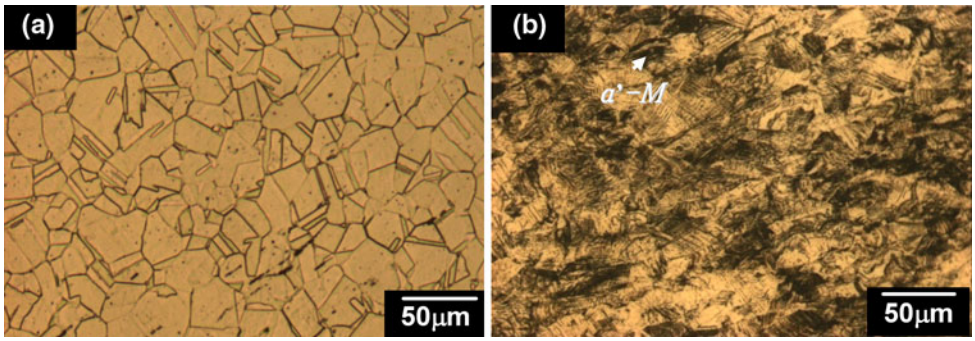

Fig. 1 Optical micrographs of 304 austenitic stainless steels, (a) annealed and (b) deformed at a room temperature with 40% reduction

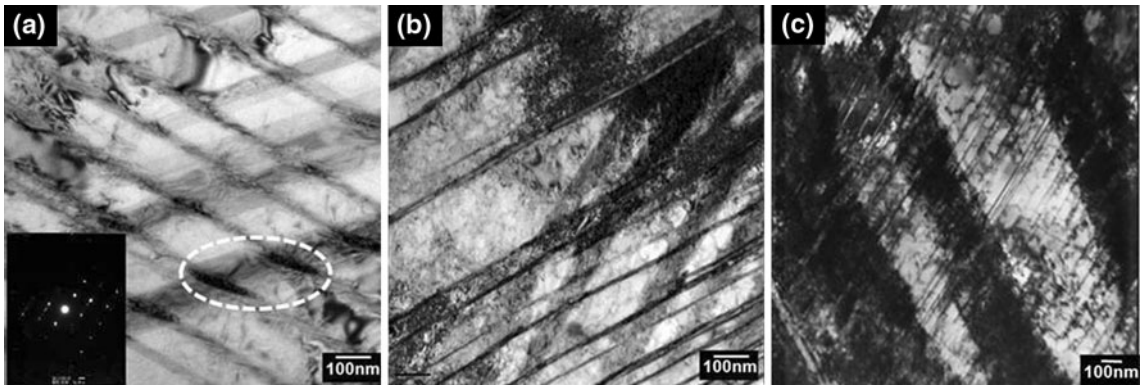

Fig. 2 TEM micrographs of 304 austenitic stainless steels, deformed at room temperature with (a) 16% reduction, (b) 29% reduction, and (c) 40% reduction

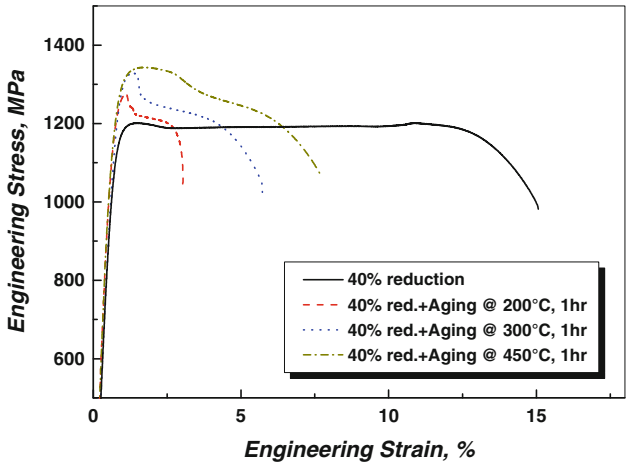

Fig. 3 Engineering stress-strain curves of 304 stainless steels, deformed 40% at room temperature, with various aging temperatures of 200-450 °C

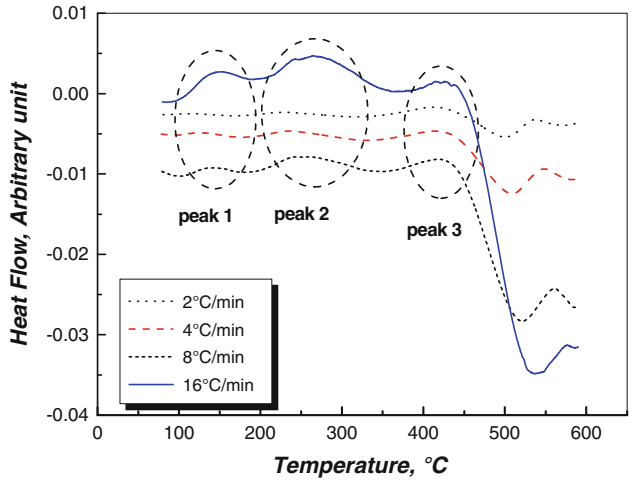

Fig. 4 DSC curves of 40% cold rolled steels, with the different heating rate of 2-16 °C/min

the temperature range of 200-450 °C are quite different from a stress-strain curve of 304 stainless steels, deformed 40%. A cold rolled steel shows the typical continuous yielding behavior with tensile strength of 1202 MPa and total elongation of 15.1%. However, an aging treatment of cold rolled steels in the temperature range of 200-450 °C, increases flow stress and decreases total elongation. In low carbon steels, the kinetics of static strain aging would be governed by the diffusion of carbon atoms to dislocations (Ref 7). The dislocations are locked by solute atmospheres and higher strain levels are required to produce free dislocations for further plastic flow. Thus, it is widely accepted that an aging treatment causes the increase of strength and the decrease of total elongation. It is interesting to note that in cold rolled and aged stainless steels (Fig. 3), both strength and total elongation increase as aging temperature increases. Accordingly, both strength and total elongation of a steel aged at 450 °C (1344 MPa, 7.7%) are much larger than those of a steel aged at 200 °C (1279 MPa, 3.0%).

3.2 Aging Kinetics

To understand microstructural evolution during aging, kinetics of strain aging were examined on cold rolled 304 stainless steels using a DSC. DSC curves in Fig. 4 reveal three exothermic peaks, representing the different stages that occurred during aging of a 304 stainless steel deformed with 40% reduction. The measured peak temperatures would be around 150 °C for the first peak, 250 °C for the second peak, and 430 °C for the third peak, respectively. Additionally, the presence of an endothermic peak around 520 °C implies that the reversion of α′-martensite to austenite would begin at a temperature above 450 °C (Ref 12).

The apparent activation energy of the peaks in Fig. 4 can give important information concerning aging mechanisms. The apparent activation energy of DSC peaks obtained by analyzing Kissinger plot would be useful to understand the mechanisms of the each stage of aging more precisely. The apparent activation energy of the first peak, 67-70 kJ/mol, is close to the activation energy for the diffusion of carbon atoms in ferrite, 66.9 kJ/mol. This means that the first peak of aging occurred at 150 °C is closely related to the diffusion of interstitial solute carbon atoms to dislocations in α′-martensite containing high

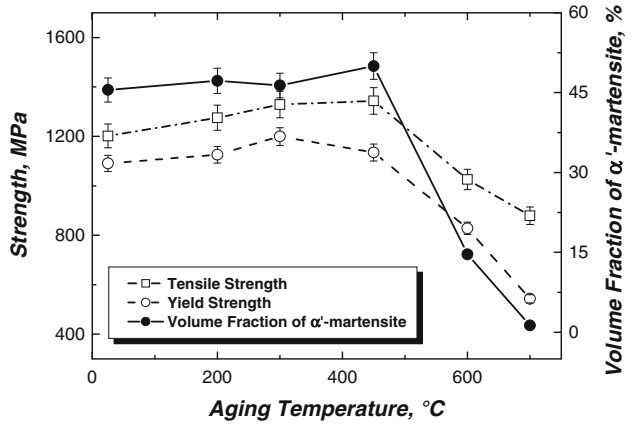

Fig. 5 Effect of aging temperature on mechanical properties and the amount of α′-martensite in cold rolled 304 stainless steels received 40% reduction. Steels were aged for an hour (Ref 16)

density of dislocations (Ref 13). Meanwhile, the apparent activation energy of the second peak, 133-138 kJ/mol, coincides with the activation energy for carbon diffusion in austenite, 134-136 kJ/mol (Ref 14). However, the measured activation energy of the third peak, 510-516 kJ/mol, seems considerably higher than the reported Q values available for steels, such as the Cr diffusion in austenite phase, 405 kJ/mol, the Cr diffusion in ferrite phase, 343 kJ/mol, the Ni diffusion in austenite phase, 280 kJ/mol, and the Ni diffusion in ferrite phase, 358 kJ/mol (Ref 15). There has been no clear explanation regarding the mechanism of the third peak. The occurrence of the third peak around 430 °C might be related to one or more of microstructural evolutions occurred at high aging temperatures, such as recovery of α′-martensite or the additional formation of α′-martensite.

3.3 Hardening Mechanisms

The variations of tensile strength, yield strength, and the amount of α′-martensite with aging temperature in cold rolled 304 stainless steels are shown in Fig. 5. Tensile strength increases continuously up to an aging temperature of 450 °C,

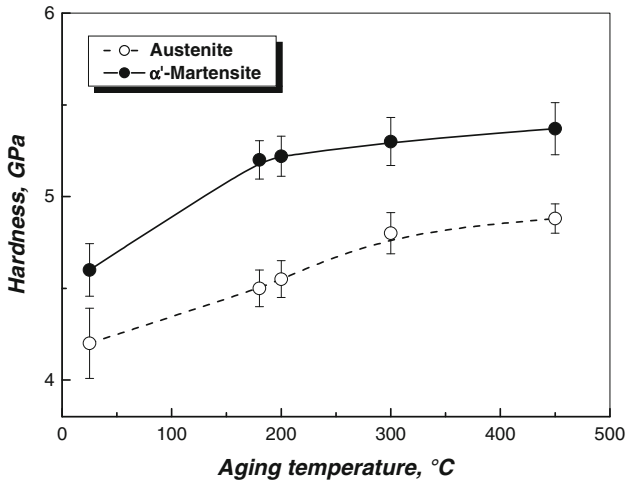

Fig. 6 The hardness of austenite and α′-martensite in 304 stainless steels cold rolled and heated to 180, 300, and 450 °C with the heating rate of 2 °C/min

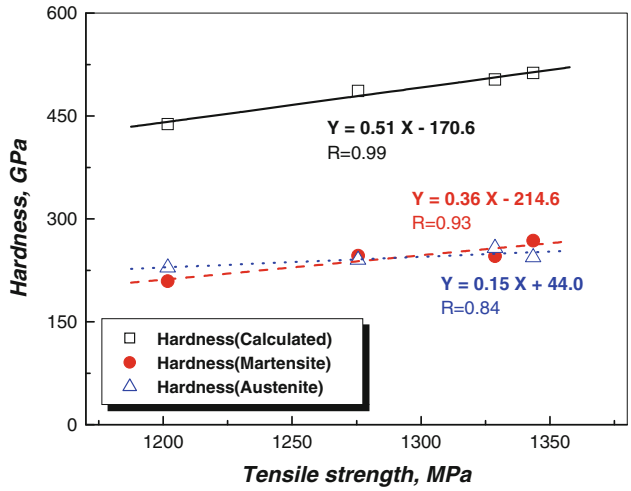

Fig. 7 The relationship between measured tensile strength and hardness of α′-martensite, hardness of deformed austenite, and calculated hardness using $H = H_{\alpha'}V_{\alpha'} + H_{\gamma}V_{\gamma}$ in cold deformed and aged 304 stainless steels

and then decreases due to the reverse transformation of α′-martensite to austenite (Ref 17), while yield strength increases up to 400 °C, and subsequently decreases with aging temperature. The similar shape of tensile strength and the amount of α′-martensite in Fig. 5 implies that there must be a relationship between the behavior of tensile strength during aging and the variation in the amount of α′-martensite. The amount of α′-martensite increases from 45.5% for a cold rolled steel to 50% for a steel cold rolled and subsequently aged at 450 °C. This increased amount of α′-martensite at the aging temperature of 450 °C would provide the evidence for the additional formation of α′-martensite (Ref 2-4) in a 304 stainless steel received 40% reduction, although its amount was less noticeable.

To understand the behaviors of austenite and α'-martensite during aging, hardness of each phase was measured using a nano-indenter (Fig. 6). Hardness of α′-martensite increases rapidly from 4.6 GPa (cold rolled) to 5.2 GPa (aged at 180 °C), while a little increase of hardness, 0.2 GPa, is found between aging temperatures of 180 and 450 °C. The rapid increase of hardness in α′-martensite up to 180 °C implies that the interaction of carbon atoms with dislocations in α′-martensite would become the main factor for the increase of hardness during low temperature aging. A decrease of hardening rate from 180 to 450 °C would be attributed to the progress of recovery in α′-martensite, in spite of hardening effect from the formation of carbide precipitates. Meanwhile, hardness of austenite increases steadily up to 300 °C. This might be related to the interaction of solute carbon atoms with dislocations or twins in deformed austenite during aging. According to Fujita et al. (Ref 6), the segregation of solute atoms on stacking faults, the Suzuki effect, can occur in a deformed and annealed 304 stainless steel. Thus, the presence of the second peak (250 °C) in Fig. 4 might be related to the segregation of solute carbon atoms to dislocations or twins in deformed austenite during aging. Accordingly, hardness of austenite would increase steadily up to 300 °C.

4. Discussion

From the above, it is obvious that the increase of tensile strength during aging would be attributed to the additional formation of α′-martensite, hardening of α′-martensite phase, and hardening of deformed austenite.

To examine the effect of the additional formation of α′-martensite on tensile strength, it is convenient to assume that tensile strength of cold deformed 304 stainless steels can be described as $\sigma = \sigma_{\alpha'\text{-martensite}}V_{\alpha'\text{-martensite}} + \sigma_{\text{austenite}}V_{\text{austenite}}$, and hardness values of α′-martensite and austenite do not change during aging. Thus, the increment of tensile strength of 140 MPa during aging at 450 °C (Fig. 5) should be closely related to the additional formation of α′-martensite, 4.5%. This means that when the amount of α′-martensite increases by 1%, tensile strength increases by 31.1 MPa. However, with the above values tensile strength of a cold rolled steel, 1202 MPa, cannot be described with the amount of α′-martensite, 45.5%. Thus, the assumption of unchanged hardness values of α′-martensite and austenite during aging, would not be proper to explain the increased tensile strength during strain aging in cold deformed and aged 304 stainless steels.

To investigate hardening of deformed austenite and α′-martensite during aging, hardness of each phase was measured using a nano-indenter. Hardness values of both α′-martensite and deformed austenite in Fig. 6 obviously increase during aging. It is also noted that the increase of hardness is more pronounced in α′-martensite than deformed austenite during aging, especially at low temperatures. This suggests that the increment of strength during aging is significantly influenced by age hardening of α′-martensite rather than deformed austenite. Thus, hardening of deformed austenite, due to the segregation of solute carbon atoms to dislocations or twins during aging (Ref 6), seems inadequate to explain the variations of tensile strength with aging time in Fig. 8.

Meanwhile, when considering that hardness values of α′-martensite and deformed austenite are varied with aging temperature and aging time, hardness of aged 304 stainless steels would be described as $H = H_{\alpha'\text{-martensite}}V_{\alpha'\text{-martensite}} + H_{\text{austenite}}V_{\text{austenite}}$. Figure 7 shows the relationship between tensile strength and hardness of α′-martensite and/or deformed austenite in cold deformed and aged 304 stainless steels. It is obvious that tensile strength of aged steels depends more significantly on the hardness of α′-martensite than the hardness

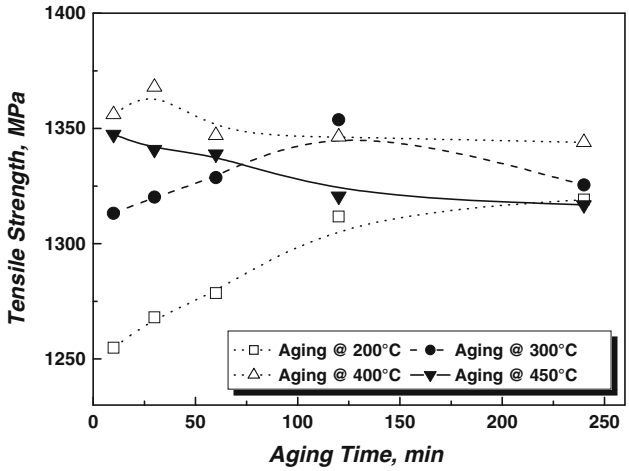

Fig. 8 Effects of aging time and aging temperature on tensile strength in cold rolled and aged 304 stainless steels

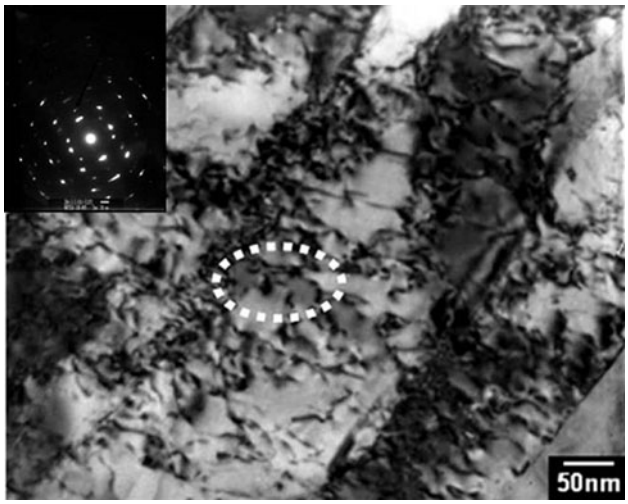

Fig. 9 A TEM micrograph, showing the presence of precipitates in a 304 stainless steel deformed with 40% reduction and aged at 450 °C for 1 h

of deformed austenite. The squares in Fig. 7 represent the sum of the contributions from volume fraction of α′-martensite, hardness of α′-martensite, and hardness of deformed austenite. However, the closest relationship between tensile strength of aged steels and the sum of the contributions described above would reflect the fact that hardening of α′-martensite and deformed austenite as well as volume fraction of α′-martensite would contribute to the hardening of cold deformed 304 stainless steels during aging.

From the above, it is obvious that the variation of tensile strength during aging would be attributed to the additional formation of α′-martensite, hardening of α′-martensite, and hardening of deformed austenite in a cold rolled 304 stainless steel. Additionally, the hardening of α′-martensite would become a major factor to increase strength during aging of a cold rolled 304 stainless steel.

Figure 8 offers the more precise information about which hardening mechanism would have the more significant influence on tensile strength of cold rolled 304 stainless steels during aging. The shapes of the aging curves in Fig. 8 are classified into two groups, depending on aging temperature. For an aging temperature of 200 °C, tensile strength increases steadily with aging time. In this case, atomic motion at a low aging temperature of 200 °C is so slow that no appreciable precipitation occurs and hardening occurs slowly. Thus, after a long time aging for 4 h tensile strength of 1319 MPa can be obtained in a steel aged at 200 °C. Thus, the increase of tensile strength with annealing time in steels aged at 200 °C would be achieved by hardening of α′-martensite and deformed austenite (as shown in Fig. 6) through the diffusion of interstitial solute atoms.

On the other hand, all of the aging curves corresponding to steels aged at temperatures above 300 °C show a tensile strength that rises to a maximum and then falls subsequently at longer aging time. The maximum tensile strength of a steel aged at 300 °C was found as 1354 MPa with annealing time of 120 min. This behavior of tensile strength with aging time and temperature resembles the typical aging curve of precipitation hardened alloys. As aging time and aging temperature increase, tensile strength increases by forming precipitates and then subsequently decreases by coarsening or over-aging of precipitates.

Meanwhile, it is worth noting that as the aging temperature is increased, the maximum in these curves moves to a shorter time. The measured aging time for the maximum tensile strength decreases as aging temperature increases, such as 120 min for 300 °C, 30 min for 400 °C, and shorter than 10 min for 500 °C. Additionally, it is also observed that as aging temperature is increased, the maximum tensile strength of aged steels increases from 1202 MPa (as deformed) up to 1368 MPa (400 °C aging) and then decreases to 1347 MPa (500 °C aging). This implies that the highest tensile strength of cold rolled 304 stainless steels during aging would be controlled by aging temperature rather than aging time.

Thus, it is expected that hardening of α′-martensite, such as the diffusion of interstitial solute carbon atoms to dislocations in α′-martensite and the precipitation of fine carbide particles, would become a major hardening mechanism in cold rolled 304 stainless steels during aging. The presence of fine carbide particles ($Cr_{23}C_6$) in Fig. 9 provides the evidence for hardening of α′-martensite phase as a major hardening mechanism in cold rolled and aged 304 stainless steels.

5. Conclusions

Age hardening of a cold rolled 304 stainless steel would be attributed to the additional formation of α′-martensite, hardening of α′-martensite, and hardening of deformed austenite. The increased amount of α′-martensite at an aging temperature of 450 °C confirmed the additional formation of α′-martensite as a hardening mechanism in a cold rolled 304 stainless steel. Additionally, the increased hardness of both α′-martensite and austenite phases with aging temperature supported hardening of both α′-martensite and austenite phases as hardening mechanisms in cold rolled and aged 304 stainless steels. Among the above hardening mechanisms, hardening of an α′-martensite phase, including the diffusion of interstitial solute carbon atoms to dislocations and the precipitation of fine carbide particles, would become a major hardening mechanism during aging in cold rolled 304 stainless steels.

Acknowledgments

This work was partially supported by Priority Research Centers Program through the National Research Foundation of Korea (NRF) funded by the Ministry of Education, Science and Technology (2009-0093814) and partially supported by the 2010 research fund of Kookmin University in Korea.

References

1. F. Gauzzi, R. Montanari, G. Principi, and M.E. Tata, AISI, 304 Steel: Anomalous Evolution of Martensitic Phase Following Heat Treatments at 400 °C, *Mater. Sci. Eng. A*, 2006, **438–440**, p 202–206
2. P.L. Mangonon and G. Thomas, Structure and Properties of Thermal-Mechanically Treated 304 Stainless, *Metall. Trans.*, 1970, **1**, p 1587–1594
3. A.N. Chukhleb and V.P. Martynov, Change in the Phase Composition of Steels of Type 18-8 in Dependence on the Temperature and the Degree of Deformation, *Met. Sci. Heat Treat.*, 1960, **1**, p 43–45
4. C.K. Mukhopadhyay, T. Jayakumar, K.V. Kasiviswanathan, and B. Raj, Study of Ageing-Induced α′-Martensite Formation in Cold Worked AISI, Type 304 Stainless Steel Using an Acoustic Emission Technique, *J. Mater. Sci.*, 1995, **30**, p 4556–4560
5. R.W. Rathbun, D.K. Matlock, and J.G. Speer, Strain Aging Behavior of Austenitic Stainless Steels Containing Strain Induced Martensite, *Scripta Mater.*, 2000, **42**, p 887–891
6. M. Fujita, Y. Kaneko, A. Nohara, H. Saka, R. Zauter, and H. Mughrabi, Temperature Dependence of the Dissociation Width of Dislocations in a Commercial 304L Stainless Steel, *ISIJ Int.*, 1994, **34**, p 697–703
7. J.R. Hämmerle, L.H. de Almeida, and S.N. Monteiro, Lower Temperatures Mechanism of Strain Aging in Carbon Steels for Drawn Wires, *Scripta Mater.*, 2004, **50**, p 1289–1292
8. J. Talonen, P. Aspegren, and H. Hänninen, Comparison of Different Methods for Measuring Strain Induced Alpha'-Martensite Content in Austenitic Steels, *Mater. Sci. Technol.*, 2004, **20**, p 1506–1512
9. R.C. Picu and D. Zhang, Atomistic Study of Pipe Diffusion in Al-Mg Alloys, *Acta Mater.*, 2004, **52**, p 161–171
10. H.E. Kissinger, Reaction Kinetics in Differential Thermal Analysis, *Anal. Chem.*, 1957, **29**, p 1702–1706
11. L.C. Chen and F. Spaepen, Analysis of Calorimetric Measurements of Grain Growth, *J. Appl. Phys.*, 1991, **69**, p 679–688
12. B.R. Kumar, A.K. Singh, B. Mahato, P.K. De, N.R. Bandyopadhyay, and D.K. Bhattacharya, Deformation-Induced Transformation Textures in Metastable Austenitic Stainless Steel, *Mater. Sci. Eng. A*, 2006, **429**, p 205–211
13. G.B. Olson and M. Cohen, Early Stages of Aging and Tempering of Ferrous Martensites, *Metall. Mater. Trans. A*, 1983, **14**, p 1057–1065
14. R.W.K. Honeycombe, *The Plastic Deformation of Metals*, 2nd ed., Edward Arnold, London, 1984, p 145
15. R.W.K. Honeycombe and H.K.D.H. Bhadeshia, *Steels—Microstructure and Properties*, 2nd ed., Edward Arnold, London, 1995, p 7
16. S.H. Lee, J.Y. Choi, and W.J. Nam, Hardening Behavior of a 304 Stainless Steel Containing Deformation-Induced Martensite During Static Strain Aging, *Mater. Trans. JIM*, 2009, **50**, p 926–929
17. B.R. Kumar, B. Mahato, N.R. Bandyopadhyay, and D.K. Bhattacharya, Influence of Strain-Induced Phase Transformation on the Surface Crystallographic Texture in Cold Rolled and Aged Austenitic Stainless Steel, *Metall. Mater. Trans. A*, 2005, **36A**, p 3165–3174